

Gas-Phase NMR Studies of *N,N*-Dimethylthioamides. Influence of the Thiocarbonyl Substituent on the Internal Rotation Activation Energies

S. M. Neugebauer Crawford, A. N. Taha, and N. S. True*

Chemistry Department, University of California, Davis, California 95616

C. B. LeMaster

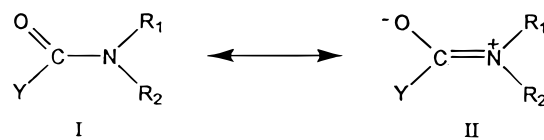
Chemistry Department, Boise State University, Boise, Idaho 83725

Received: March 17, 1997; In Final Form: May 2, 1997[⊗]

Temperature-dependent gas-phase ¹H NMR spectra of seven thiocarbonyl-substituted *N,N*-dimethylthioamides (YCSN(CH₃)₂) obtained at 300 MHz are consistent with the following free activation energies Δ*G*₂₉₈[‡] (kcal mol⁻¹): Y = H, 22.5 (0.1); CH₃, 18.0 (0.1); F, 18.3 (0.1); Cl, 16.9 (0.2); CF₃, 17.2 (0.1); CH₂CH₃, 17.6 (0.1); CH(CH₃)₂, 16.3 (0.1). The results are compared to condensed-phase values and to the corresponding gas-phase oxoamides.

Introduction

The rotational barrier in amides and thioamides has been the focus of substantial investigation. Much of this attention stems from the importance of amide functional groups in biologically important systems as the building blocks of proteins and enzymes.¹ The planar structure and relatively high barrier to rotation about the C–N bond are considered to be important influences in determining stable protein conformation and the secondary and tertiary structure linked to biological activity. The high barrier to rotation about the C–N bond in amide systems has been explained using a simple resonance model in which resonance form II contributes partial double-bond character to the ground state and subsequently inhibits free C–N bond rotation. The effect of the substituted carbonyl group on amide internal rotation is explained predominately in terms of lone-pair stabilization and changes in electronegativity.² The role of oxygen is simply to cause polarization of the C=O bond, which leads to an electron-deficient carbon atom. Thus, in the planar ground state, the nitrogen atom has the opportunity to minimize the energy of its lone-pair electrons through interaction with this electron-deficient carbonyl carbon. For this interaction to take place, the lone pair must occupy a p orbital, which results in sp² hybridization of the nitrogen atom. Upon 90° C–N bond rotation, this interaction is lost and rehybridization occurs. Nitrogen, in an attempt to stabilize its lone pair as much as possible, places it in an orbital of higher s character (increasing the atoms' electronegativity and bringing the electronic charge closer to the nucleus), resulting in sp³ hybridization and a corresponding loss of planarity. This model of amide rotation has been quite successful in describing the observed carbonyl substituent effects on amide rotational barriers.³ In general, carbonyl substituents larger than Y = H lower the barrier to rotation by destabilizing the planar ground state due to R–Y crowding. Because the carbonyl carbon is more electron deficient in the transition state than in the ground state, effects of electron-donating and -withdrawing substituents are described in terms of their stabilization and destabilization of the transition-state structure.



Although thioamide systems have been studied to a much lesser degree than their carbonyl counterparts, the existing data have consistently shown the rotational barriers to be higher (≈ 2 kcal mol⁻¹) than for their amide analogs.^{4–15} The origin of this increased barrier has been the focus of several experimental and theoretical queries.^{10,12,16–21} Initially, the higher barrier was explained by the reluctance of second-row elements to form double bonds, as required in the classical transition-state picture of amide C–N bond rotation. More recently, Wiberg and Rablen¹⁷ reported theoretical results suggesting that the interactions in thioformamide are different from those in formamide because of the substitution of the relatively nonpolar C=S group for the highly polar C=O group. They explain that the nitrogen-to-carbonyl-carbon interaction, important in amides due to the electron-deficient character of the carbonyl carbon, is not important in thioformamide, but it is replaced by a charge-transfer interaction between nitrogen and sulfur. The increased size and predominately uncharged nature of the sulfur atom makes it capable of accepting considerable charge from nitrogen. Theoretical calculations with geometry optimization at the MP2/631+G* level of theory indicate that there is about twice the amount of charge transfer in thioformamide as in formamide. This “greater amide resonance” leads to more stabilization of the thioamide than the oxoamide ground-state structure, thus a higher barrier for thioamides. Laidig and Cameron¹⁸ challenge this interpretation, suggesting that the resonance model is not needed to explain hindered rotation in amides. It is the preference of the amide nitrogen to remain planar, therefore better able to withdraw charge from its neighbor atoms, that creates the rotational barrier in both thio- and oxoamides. Their theoretical calculations using HF/6-311++G** optimized wave functions indicate that there is no significant charge transfer from nitrogen to either oxygen or sulfur in the ground state. Thus, resonance structure II contributes little to amide stability. Instead, they conclude that the changes that occur upon rotation of the C–N bond are similar in both oxo- and thioamides and can be better understood by viewing amides as (thio)-

[⊗] Abstract published in *Advance ACS Abstracts*, June 15, 1997.

TABLE 1: Systems Studied

Y =	X = O	X = S
H	DMF	DMTF
CH ₃	DMA	DMTA
CH ₂ CH ₃	DMP	DMTP
CH(CH ₃) ₂	TMP	TMTP
F	DMCF	DMTCF
Cl	DMCCI	DMTCCI
CF ₃	DMCF ₃	DMTCF ₃

formylamines. They suggest that the thioamides have higher barriers because there is greater donation of charge from the thioformyl group to the more electronegative nitrogen than there is from the formyl group. This increases the energy requirement for the rehybridization of nitrogen in the transition state.

The present study examines the effect on the rotational barrier of altering the steric and electronic character of the thiocarbonyl carbon substituent in a series of thioamides and compares these results with the substituent effects observed on the rotational barrier in their oxoamide analogs. It is not unreasonable to expect to observe considerable differences in the influence of substituents on the rotational barrier between these two classes of amides because there is considerable difference in polarity and size of the C=X moiety. Although a considerable number of amide and thioamide barriers have been determined from NMR experiments, the great majority of these have been determined by solution-phase experiments. It is well-known that liquid barriers are consistently higher than gas-phase barriers in amide systems where amide self-association, solvation differences between the ground and transition state, and solvent internal pressure can affect the rotation rate and mask or disguise the intrinsic influence of substituents.²² On the other hand, gas-phase barriers, although more difficult to obtain experimentally, lend themselves more readily to the analysis of trends, reveal intrinsic molecular features, and are better compared to theoretical values, which generally examine isolated molecules. We present the gas-phase kinetic parameters from variable-temperature NMR studies for a systematic series of *N,N*-dimethylthioamides (Table 1) and compare them to the gas-phase values obtained previously for their amide analogs.

Experimental Section

Synthesis of *N,N*-Dimethylthiocarbonyl Fluoride. *N,N*-Dimethylthiocarbonyl fluoride (DMTCF) was prepared by slowly adding 18 g of powdered silver fluoride (Strem Chemicals) to 13.9 g of tetramethylthiuram disulfide (Aldrich) dissolved in 100 mL of cooled (30–40 °C) acetonitrile.²³ The mixture was stirred for an additional 30 min maintaining the temperature between 30 and 40 °C. The acetonitrile was removed with a rotary evaporator and the residue washed with ether and filtered. The ether was removed, and the remaining residue was vacuum distilled. The resulting *N,N*-dimethylthiocarbonyl fluoride was characterized by NMR and IR spectroscopy.

Synthesis of *N,N*-Dimethylthiotrifluoroacetamide. *N,N*-Dimethyltrifluoroacetamide (DMCF₃) carbonyl precursor was prepared by slow addition of a molar excess of trifluoroacetic anhydride (Aldrich) to condensed anhydrous dimethylamine (Matheson) at 0 °C. The resulting solution was washed with saturated sodium bicarbonate and diethyl ether. The ether was

removed to yield pure *N,N*-dimethyltrifluoroacetamide, which was converted to the thionyl analog by stirring over a 0.25 molar ratio of phosphorus pentasulfide (Acros Chemical) in xylene. The resulting mixture was filtered and washed with water. Removal of the xylene produced the product *N,N*-dimethylthiotrifluoroacetamide (DMTCF₃), which was characterized by ¹H NMR.

Synthesis of *N,N*-Dimethylthiopropionamide and *N,N*,2-Trimethylthiopropionamide. The thio analogs of *N,N*-dimethylpropionamide (DMP) and *N,N*,2-trimethylpropionamide (TMP) were prepared by slow addition of phosphorus pentasulfide (Acros Chemical) to a hot solution of each amide (Aldrich) in xylene, which was subsequently stirred with continued warming for 2–3 h.²⁴ The resulting mixtures were filtered and washed with water and ether. Removal of the ether and xylene gave the thioamide analogs: *N,N*-dimethylthiopropionamide (DMTP) and *N,N*,2-trimethylthiopropionamide (TMTP), which were characterized by ¹H NMR spectroscopy.

Sample Preparation. The remaining thioamides, *N,N*-dimethylthioformamide (DMTF, Aldrich), *N,N*-dimethylthiocarbonyl chloride (DMTCCl, Aldrich), and *N,N*-dimethylthioacetamide (DMTA, ICN), were obtained commercially and used without further purification. Gas-phase NMR samples were prepared in restricted-volume NMR tubes constructed from 3-cm-long sections of Wilmad high-precision 12-mm coaxial inserts. The short tubes were inserted into longer 12-mm tubes for introduction into the probe. The short tubes confined the sample and reduced the temperature gradient within the active volume. Samples were prepared by depositing a small drop or a tiny crystal (DMTA) in the bottom of the sample tube. At least 30 Torr of Me₄Si (frequency and resolution reference) and 300 Torr of argon (to inhibit oxidation of the samples with heating and to ensure first-order kinetics) were then added to the slightly cooled 3-cm insert tube before sealing. The thioamide gas equilibrates at its vapor pressure, which increases as the probe temperature is raised. This technique allows the sample vapor pressure and thus the NMR signal to increase with temperature. Samples were run from low to high temperature to avoid condensation on the walls of the insert tube within the active volume. The absence of liquid signals in the spectra, which characteristically appear upfield from the gaseous resonance signals, is evidence that condensation was not present within the active volume of the probe.

Spectroscopy. Gas-phase ¹H NMR spectra were acquired on a wide-bore GE NT-300 spectrometer (proton observation at 300.06 MHz) fitted with a Tecmag acquisition upgrade and equipped with a Bradley 12-mm proton probe. All measurements were made on spinning samples in unlocked mode. Acquisition time was 1.0 s per transient with a 1.0 s delay time and a 90° flip angle (pulse length = 14 μs). Typically, 1000–4000 transients were collected at each temperature and stored in 8K of memory to achieve a minimum signal to noise ratio of 10:1 after multiplication by an exponential line-broadening factor of 1 Hz. Sweep width was ±2500 Hz giving a digital resolution of 0.6 Hz/point. Temperatures were controlled with a 0.1 °C pyrometer and read after each acquisition. Temperature measurements for the gas-phase spectra were made using two copper-constantan thermocouples placed within an empty 3-cm-long 12-mm-o.d. insert tube, which was placed within a 12-mm NMR tube. This arrangement closely resembles the sample system. In this manner the temperature gradient within the active volume of the probe was found to be less than 0.2 K for most acquisition temperatures. Samples were allowed to thermally equilibrate at each temperature for at least 10 min prior to initiating the acquisition.

TABLE 2: Rate Constants (*k*) for Internal Rotation in Gaseous *N,N*-Dimethylthioamides as a Function of Temperature

DMTF		DMTA		DMTCF		DMTCCI		DMTCF ₃		DMTP		TMTP	
<i>T</i> (K)	<i>k</i> (s ⁻¹)	<i>T</i> (K)	<i>k</i> (s ⁻¹)	<i>T</i> (K)	<i>k</i> (s ⁻¹)	<i>T</i> (K)	<i>k</i> (s ⁻¹)	<i>T</i> (K)	<i>k</i> (s ⁻¹)	<i>T</i> (K)	<i>k</i> (s ⁻¹)	<i>T</i> (K)	<i>k</i> (s ⁻¹)
410.4	8.3(0.5)	342.4	19.4(0.8)	323.5	2.3(0.7)	308.7	7.0(0.4)	311.1	5.4(0.5)	347.2	63.5(1.2)	313.0	25.7(1.5)
415.0	10.7(0.5)	346.8	25.0(0.6)	327.5	3.8(0.3)	311.2	8.7(0.7)	313.1	6.8(0.5)	348.9	70.6(1.0)	315.0	31.5(1.9)
418.1	14.3(0.3)	350.3	30.2(0.6)	336.9	8.9(0.6)	313.3	14.6(0.5)	315.1	7.9(0.4)	350.7	73.7(0.6)	317.0	34.5(0.9)
422.4	17.5(0.6)	353.9	36.5(1.0)	341.4	12.5(0.2)	318.1	15.7(0.4)	316.1	8.8(0.4)	352.2	80.5(0.8)	319.0	40.5(1.0)
427.6	22.3(0.5)	357.3	48.3(0.7)	345.5	13.2(1.3)	321.1	21.6(0.3)	317.2	9.4(0.4)	353.0	91.9(0.9)	321.1	52.2(0.7)
429.3	28.8(0.3)	357.9	53.9(0.5)	349.9	20.9(0.3)			319.3	12.3(0.5)	354.1	104.2(1.1)	322.9	55.2(1.0)
432.7	33.9(0.4)	360.9	64.3(0.8)	354.4	29.3(0.3)			320.1	12.4(0.3)	356.2	119.2(0.9)	324.7	65.2(0.8)
434.8	37.9(0.3)	362.3	77.1(0.5)	357.9	33.2(0.5)			321.1	13.0(0.4)	357.2	126.9(1.2)	326.7	72.5(1.0)
435.8	42.1(0.3)	364.3	84.3(0.5)	361.5	44.2(1.0)			322.1	15.3(0.3)			328.7	83.0(1.7)
437.8	48.2(0.3)	367.2	105.9(0.5)	364.2	51.5(0.5)			323.9	18.2(0.5)			330.5	106.2(2.0)
		368.8	126.7(0.8)	365.8	55.4(0.5)			325.9	20.0(0.4)				
		370.9	129.4(0.5)	367.2	63.4(0.8)								
		374.5	151.6(0.8)	368.8	84.7(0.5)								
				370.9	99.9(0.5)								
				372.9	119.8(0.6)								

Parameter Determination. Rate constants were calculated for exchanging spectra by using the computer program DN-MR5,²⁵ which uses an iterative nonlinear least-squares regression analysis to obtain the best fit of the experimental NMR spectrum. For each gaseous amide, spectra were analyzed as uncoupled A₃X₃ systems. The effective line-width parameter was measured at slow and fast exchange for each amide when possible. Fast-exchange spectra could not be obtained for DMTF because fast-exchange temperatures were beyond the temperature limits of the probe. The effective line width was estimated at each temperature by assuming a linear temperature dependence. The line width of Me₄S was used to estimate the magnetic field inhomogeneity contribution to the line width at each temperature. This factor and the exponential line-broadening factor were added to the interpolated values for the effective line width to obtain the total line broadening and thus the effective transverse relaxation time (*T*₂) at each temperature where rates were determined. The line width of the acetomethyl group in DMTA provided an additional measure of the effective line width throughout the exchanging temperature range. Spectra were analyzed by iterating on the rate constant, spectral origin, base-line height, and base-line tilt. All other parameters were held constant.

Results

Table 2 lists the complete sets of rate constants (and their standard errors) used to determine the gas-phase activation parameters for all the dimethylthioamides studied. Figure 1 shows a graphical representation of the rates in the form of Eyring plots for each thioamide system. The experimental activation parameters obtained for the gaseous systems are given in Table 3. Specific observations for each amide studied are described below.

***N,N*-Dimethylthioformamide.** The ¹H methyl resonances of gaseous DMTF were observed 3.11 ppm downfield from gaseous Me₄Si with a limiting chemical shift separation of 0.095 ppm (28.80 Hz in a 7.05 T magnetic field) at 350.25 K. Exchange-broadened spectra were obtained over a temperature range from 415.1 to 422.4 K. No evidence of any chemical shift temperature dependence was observed, as evidenced by constant chemical shift values throughout the slow-exchange temperature range (308–383 K). The formyl proton resonance was observed 9.33 ppm downfield from gaseous Me₄Si. Fast-exchange spectra were not obtained for this system due to instrumental temperature limitations (*T* > 473 K).

***N,N*-Dimethylthioacetamide.** The ¹H methyl resonances of gaseous DMTA were observed 3.254 ppm downfield from gaseous Me₄Si with a limiting chemical shift separation of 0.245

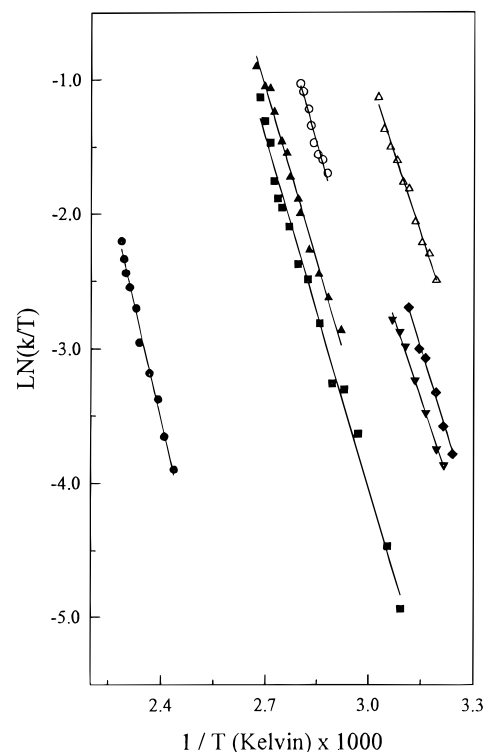


Figure 1. Eyring plots of gas-phase exchange rate constants for *N,N*-dimethylthioamides: (●) DMTF; (▲) DMTA; (■) DMTCF; (◆) DMTCCl; (△) TMTP; (○) DMTP; (▼) DMTCF₃.

TABLE 3: Thermodynamic Parameters for Gas-Phase Internal Rotation in *N,N*-Dimethylthioformamide (DMTF), *N,N*-Dimethylthioacetamide (DMTA), *N,N*-Dimethylthiocarbonyl Fluoride (DMTCF), Dimethylthiocarbonyl Chloride (DMTCCI), *N,N*-Dimethylthiotrifluoroacetamide (DMTCF₃), *N,N*-Dimethylthiopropionamide (DMTP), and *N,N*,2-Trimethylpropionamide (TMTP)

	ΔG^\ddagger_{298} (kcal/mol)	ΔH^\ddagger (kcal/mol)	ΔS^\ddagger (cal/(mol K))
DMTF	22.5(0.1)	22.3(1.5)	-0.7(2.5)
DMTA	18.0(0.1)	17.1(1.0)	-3.3(2.0)
DMTCF	18.3(0.1)	17.2(1.2)	-3.0(3.0)
DMTCF ₃	17.2(0.1)	17.2(1.1)	-0.1(3.0)
DMTCCI	16.9(0.1)	16.8(1.3)	-0.2(4.0)
DMTP	17.6(0.1)	17.4(2.5)	-0.6(5.0)
TMTP	16.30(0.1)	15.5(1.0)	-2.6(3.0)

ppm (73.52 Hz in a 7.05 T field). The acetomethyl proton resonance was observed 2.530 ppm downfield from gaseous Me₄Si. Again, as for DMTF, no temperature dependence of the chemical shifts was observed. Exchange-broadened spectra were obtained over the temperature range 342.4–374.5 K.

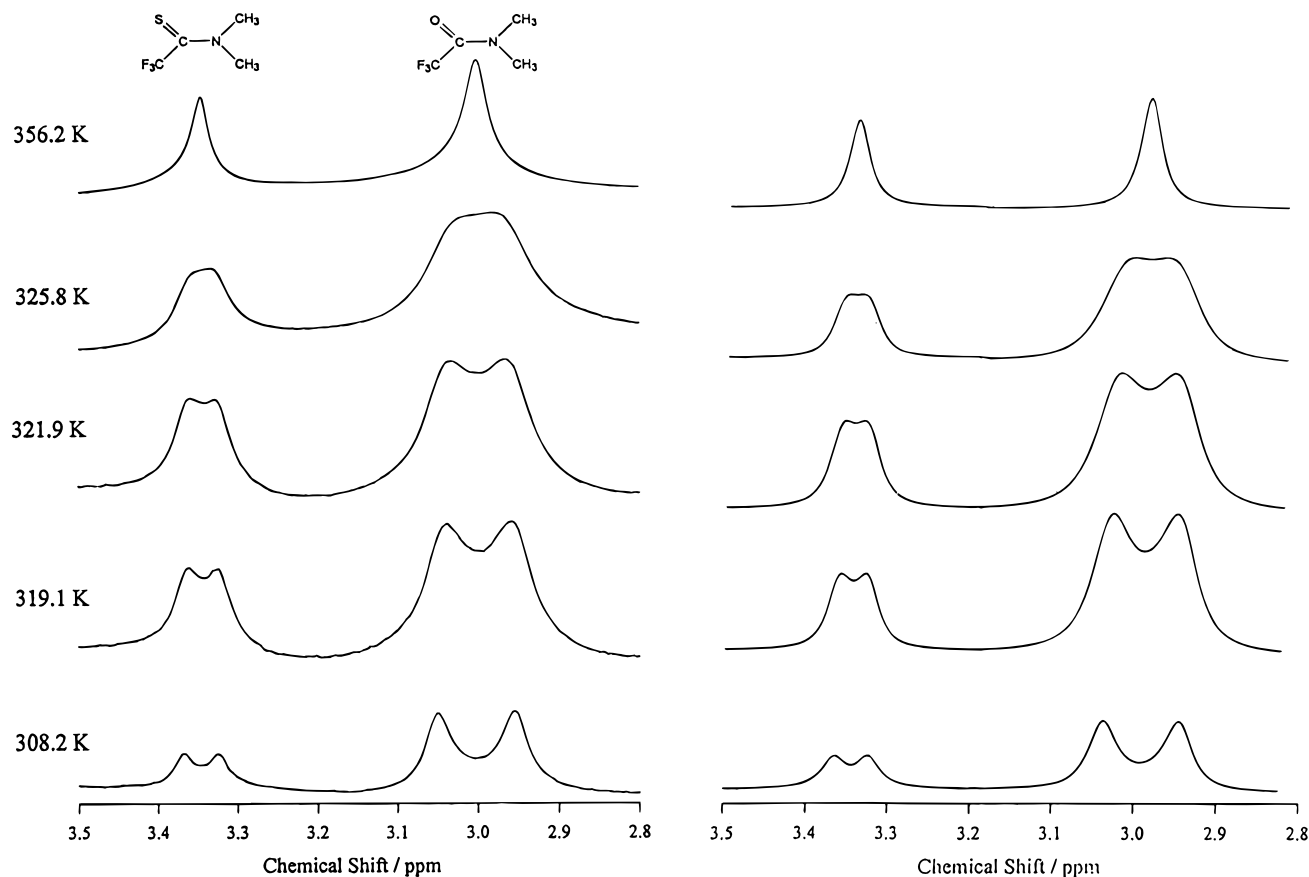


Figure 2. (a) Experimental (left) and (b) calculated (right) temperature-dependent gas-phase 300-MHz ¹H NMR spectra of the *N*-methyl protons in *N,N*-dimethylthio-*N,N*-dimethyltrifluoroacetamide and *N,N*-dimethyltrifluoroacetamide.

***N,N*-Dimethylthio-*N,N*-dimethyltrifluoroacetamide.** The ¹H methyl resonances of gaseous DMTTCF₃ were observed 3.340 ppm downfield from gaseous Me₄Si with a limiting chemical shift separation of 0.042 ppm (12.60 Hz in a 7.05 T field). An additional pair of signals (doublet) was observed 2.995 ppm downfield from gaseous Me₄Si with a limiting chemical shift separation of 0.096 ppm (28.80 Hz in a 7.05 T field). These signals were assigned to the ¹H methyl resonances of the oxo analog impurity *N,N*-dimethyltrifluoroacetamide. This assignment was based on their chemical shift, observed coalescence at 336 K, and an activation free energy for rotation of 16.4 kcal mol⁻¹, which agrees well with the results previously obtained for *N,N*-dimethyltrifluoroacetamide (16.3 kcal mol⁻¹) by Ross, True, and Decker.²⁶ The exchange-broadened spectra for gaseous DMTTCF₃ were obtained over the temperature range from 310 to 330 K. Figure 2a shows the experimental gas-phase variable-temperature ¹H spectra of the aminomethyl proton resonances for both the carbonyl (higher field) and thionyl *N,N*-dimethyltrifluoroacetamide derivatives. The calculated spectra are shown in Figure 2b.

Additionally, solution-phase exchange data were obtained for neat DMTTCF₃ and for a 1% solution in tetrachloroethane (TCIE). At slow exchange (301 K), methyl resonances were observed at 2.937 and 2.824 ppm in the neat liquid and at 3.361 and 3.302 ppm ($\Delta\nu = 17.70$ Hz) in the 1% TCIE solution (downfield from liquid Me₄Si). The higher field resonance in each case was resolved into a quartet ($J = 1.2$ Hz), and the lower field resonance was observed to be broadened with signs of incompletely resolved structure. This splitting was assigned to long-range fluorine coupling. The neat chemical shifts showed a temperature dependence of 1.78×10^{-4} ppm K⁻¹ for the higher field resonance and 1.64×10^{-4} ppm K⁻¹ for the lower field resonance. An analogous temperature dependence was absent

in the 1% TCIE solution. The spectra of both solution samples contained evidence of the carbonyl impurity *N,N*-dimethyltrifluoroacetamide, showing methyl resonances at 3.082 and 3.014 ppm ($\Delta\nu = 20.40$ Hz) at slow exchange. It is interesting to note that the carbonyl resonances appear reversed with respect to the thio analog, with the lower field resonance showing increased fluorine long-range coupling ($J = 1.5$ Hz) in the carbonyl amide's spectra. Exchange data for the solution-phase spectra (neat and 1% in TCIE) were obtained over the temperature range 363–383 K ($T_c \approx 379$ K). Fitting of these liquid spectra was accomplished with inclusion of the fluorine long-range coupling. The thermodynamic parameters for internal rotation determined through analysis of the rates obtained from total line-shape analysis are $\Delta G^\ddagger_{298} = 19.5(0.1)$ kcal mol⁻¹, $\Delta H^\ddagger = 20.5(1.8)$ kcal mol⁻¹, and $\Delta S^\ddagger = 3.2(6.0)$ cal mol⁻¹ K⁻¹.

***N,N*-Dimethylthio-*N,N*-dimethylpropionamide and *N,N*-Dimethylpropionamide.** The ¹H slow-exchange spectra of gaseous DMTP consist of a triplet at 1.23 ppm ($J = 6$ Hz), a quartet at 2.62 ppm ($J = 3$ Hz), and two singlets centered at 3.282 ppm with a limiting chemical shift separation of 0.233 ppm ($\Delta\nu = 69.9$ Hz in a 7.05 T field). Exchange-broadened spectra were obtained over the temperature range from 347 to 357 K.

The solution-phase slow-exchange spectra of DMTP (1% in TCIE) consist of a triplet at 1.25 ppm ($J = 12$ Hz), a quartet at 2.697 ppm, and two singlets assigned to the slow-exchange methyl resonances centered at 3.262 ppm with a limiting chemical shift difference of 0.242 ppm ($\Delta\nu = 72.61$ Hz in a 7.05 T field), all downfield from Me₄Si. Solution-phase exchange-broadened spectra were obtained over the temperature range from 397 to 409 K. The resulting thermodynamic parameters for internal rotation in dilute TCIE solution were $\Delta G^\ddagger_{298} = 20.7(0.1)$ kcal mol⁻¹, $\Delta H^\ddagger = 21.5(2.0)$ kcal mol⁻¹, and $\Delta S^\ddagger = 2.5(6.0)$ cal mol⁻¹ K⁻¹.

TABLE 4: Comparison of ΔG^\ddagger (kcal/mol) for Internal Rotation in Liquid and Gas-Phase *N,N*-Dimethylamides and *N,N*-Dimethylthioamides (YC(X)N(CH₃)₂)

Y	gas				liquid					
	X = O	ref	X = S	ref	X = O	solvent	ref	X = S	solvent	ref
H	19.4(0.1)	47	22.5(0.1)	6	20.9	neat	40	25.5	neat	6
			22.5		21.3	neat	41	23.5	decalin	6
					21.2	formamide	42	24.2	DCIB	6
					20.9	TCIE	43	24.1	DCIB	13
					22.4	neat	44			
CH ₃	15.7(0.1) 15.6(0.1)	33 7	18.0(0.1)	6	17.33	CCL ₄	45	21.6	DCIB	10
			18.0(0.1)		17.3	isooctane	41	24.1	formamide	42
					18.1	neat	46	21.8	theoretical	20
					18.5	DCIB	13	20.3	decalin	41
					20.1	neat	44			
F	17.1(0.1) 17.1(0.2)	7	18.3(0.1)		18.1(0.6)	CCL ₄	37	20.7(0.5)	TCIE	9
Cl	15.4(0.2) 15.4	35 7	16.9(0.1)		16.5(0.5)	CCL ₄	36	19.	CCL ₄	8
					16.8(0.5)	neat	36	19.1	DCIB	10
					16.8	neat	8			
					16.3	CCL ₄	8			
CF ₃	16.4(0.1) 16.5(0.1)	26 7	17.2(0.1)		19.5	neat	44	19.8(0.2)	neat	
					17.8	CCL ₄	26	19.5(0.1)	TCIE	
					18.1	CCL ₄	45			
					17.4	CCL ₄	49			
CH ₂ CH ₃	<i>a</i>		17.6(0.1)		16.6	CCL ₄	49	20.7(0.1)	TCIE	
					17.4	CCL ₄	49			
					17.6	neat	49			
CH(CH ₃) ₂	14.3 ^b		16.3(0.1)		17.0(0.1)	acetone	48			
					16.2	DCIB	15	19.3	DCIB	41
							19.1(0.1)	TCIE		

^a Not obtainable due to isochronicity of *N*-methyl resonances. ^b Calculated from observed limiting chemical shift difference and coalescence temperature. DCIB (dichlorobenzene). TCIE (tetrachloroethane).

Thermodynamic parameters were not obtained for gaseous *N,N*-dimethylpropionamide due to chemical shift isochronicity of the methyl resonances observed down to 273 K. This is consistent with previous findings by the True group.²⁷

***N,N,N*-Trimethylthiopropionamide and *N,N,N*-Trimethylpropionamide.** The ¹H NMR spectrum of gaseous TMTP at 303 K consists of a doublet at 1.23 ppm, a weak broad signal at 3.1 ppm, and two singlets centered at 3.31 ppm with a limiting chemical shift difference of 0.20 ppm ($\Delta\nu = 59.1$ Hz in a 7.05 T field), which are assigned to the two *N*-methyl resonances at slow exchange. Exchange-broadened spectra were collected over the temperature range from 313 to 333 K.

The solution-phase ¹H spectrum of 1% TMTP in TCIE consists of a doublet at 1.19 ppm ($J = 6$ Hz), a septet at 3.12 ppm, and two slow-exchange methyl resonance singlets centered at 3.35 ppm with a limiting chemical shift difference of 0.16 ppm ($\Delta\nu = 48.01$ Hz in a 7.05 T field). Exchange-broadened spectra were obtained over the temperature range from 373 to 390 K. The activation parameters for internal rotation in dilute TCIE solution are $\Delta G^\ddagger_{298} = 19.1(0.1)$ kcal mol⁻¹, $\Delta H^\ddagger = 17.4(1.5)$ kcal/mol, and $\Delta S^\ddagger = -5.7(4)$ cal K⁻¹ mol⁻¹.

The slow-exchange spectrum of gaseous *N,N,N*-trimethylpropionamide at 268 K consists of a doublet at 1.092 ppm assigned to the isopropyl methyls and two singlets centered at 2.932 ppm with a limiting chemical shift difference of 0.081 ppm ($\Delta\nu = 24.31$ Hz in a 7.05 T field) assigned to the *N*-methyl resonances. The resonance for the methine proton was not observed due to poor signal to noise at slow-exchange temperatures. The inability to obtain gaseous exchange-broadened spectra of sufficient quality for fitting due to the low sample volatility at exchange temperatures ($T_c = 283$ K) necessitated the estimation of the rotational barrier for this molecule. The barrier was calculated using the observed limiting chemical shift difference and coalescence temperature.

***N,N*-Dimethylthiocarbamoyl Fluoride.** The ¹H methyl resonances of gaseous DMTCF were observed 3.122 ppm downfield from gaseous Me₄Si with a limiting chemical shift

separation of 0.224 ppm (67.21 Hz in a 7.05 T magnetic field). An additional signal (singlet) was observed 2.852 ppm downfield from Me₄Si. This signal broadened and decoalesced into two singlets at ca. 313 K. The chemical shift and observed decoalescence of this signal suggest that it may be due to the impurity *N,N*-dimethylcarbonyl fluoride. Exchange-broadened gas-phase spectra for these additional signals were obtained and analyzed by line-shape analysis. Analysis of the rate constants obtained yielded a free energy for rotation about the C–N bond of 17.1(0.1) kcal mol⁻¹. This value compares with the free energy of 17.1(0.2) kcal mol⁻¹ previously obtained by Feigel⁷ for gaseous *N,N*-dimethylcarbonyl fluoride. Similarly, the liquid-phase spectra of DMTCF in CDCl₃ at 298 K also exhibited the decoalesced oxygen-analog methyl signals at 3.316 (singlet) and 3.159 ppm (doublet, $J = 2.1$ Hz) and an additional pair of impurity signals (two singlets) at 2.956 and 2.964 ppm. The lower field signal appeared broadened, as would be expected for the oxygen analog due to the stronger fluorine coupling. These signals coalesced at ca. 333 K.

***N,N*-Dimethylthiocarbamoylchloride.** The ¹H slow-exchange spectra (≈ 300 K) of gaseous DMTCI consist of two resonances (singlets) of equal intensity centered at 3.363 ppm with a limiting chemical shift difference of 0.062 ppm ($\Delta\nu = 18.60$ Hz in a 7.05 T field) downfield from gaseous Me₄Si. Exchange-broadened spectra were obtained between 308 and 321 K. Coalescence was observed at approximately 323 K. The low sample volatility of this system combined with the low temperature for the exchange region required an extensive number of scans (up to 30 000 at some temperatures) to obtain spectra with signal to noise adequate for fitting.

Discussion

Table 4 summarizes the gas-phase activation free energy, ΔG^\ddagger_{298} , for internal rotation in seven dimethylthioamides and oxoamides and selected liquid values for comparison. Several more complete compilations of liquid-phase barriers are avail-

TABLE 5: Changes in Gas-Phase $\Delta G^{\ddagger}_{298}$ (kcal/mol) with (Thio)carbonyl Substituent Y ($\Delta\Delta G^{\ddagger} = \Delta G^{\ddagger}_{(\text{formamide;thioformamide})} - \Delta G^{\ddagger}_{(\text{amide;thioamide})}$)

Y	oxoamide (X = O)		thioamide (X = S)	
	$\Delta G^{\ddagger}_{298}$	$\Delta\Delta G^{\ddagger}_{298}$	$\Delta G^{\ddagger}_{298}$	$\Delta\Delta G^{\ddagger}_{298}$
H	19.4	0	22.5	0
CH ₃	15.7	3.6	18.0	4.5
CH ₂ CH ₃			17.6	4.9
CH(CH ₃) ₂	14.3	5.1	16.3	6.2
F	17.1	2.3	18.3	4.2
Cl	15.4	4.0	16.9	5.6
CF ₃	16.4	3.0	17.2	5.3

able.^{3,28,29} Table 5 lists gas-phase differences in $\Delta G^{\ddagger}_{298}$ relative to DMF and DMTF, which have the highest rotational barrier for the *N,N*-dimethyloxo- and *N,N*-dimethylthioamides, respectively. The data in Tables 4 and 5 show similarities and differences between oxo- and thioamides which can be compared to predictions based on the three models for the origin of the rotational barriers discussed in the Introduction. We will refer to the simple resonance model as model 1, the extended resonance model¹⁷ as model 2, and the (thio)formylamine model¹⁸ as model 3.

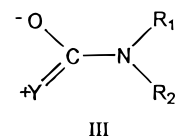
Similarities include the general observation in Table 4 that $\Delta G^{\ddagger}_{298}$'s are lower (by 2–4 kcal mol⁻¹) in the gas phase than in the liquid phase for both oxo- and thioamides. This has been attributed to the added internal pressure in the liquid and a transition state with greater steric requirements than the ground state.³⁰ This observation does not contradict any of the three models. Close inspection of the liquid data illustrates the variability of the values obtained in liquids for any given species. The solution barriers are dependent on solvent and concentration. Generally, high solvent polarity and high amide concentrations raise the rotation barrier. (This medium dependence has been examined and compared to gas-phase values for several amides and thioamides.^{7,26,30–33}) Since intrinsic effects on structure and reactivity may be masked by solvent effects in liquids, gas-phase studies are better suited to examine subtle kinetic and thermodynamic effects of substituents. The discussion below focuses on the gas-phase results.

Thioamide barrier heights are consistently higher than those of their oxoamide analogs in both gases and liquids. This is adequately explained by models 2 and 3 but not by model 1. Model 3¹⁷ predicts higher barriers for thioamides due to the greater donation of charge to the amido group by the more polarizable C=S compared to C=O. This makes the rehybridization of nitrogen, required for rotation, more costly in thioamides. Model 2¹⁸ attributes the higher barriers to greater charge transfer from nitrogen to sulfur than to oxygen, which is facilitated by the small difference in electronegativity between carbon and sulfur and the larger size of the sulfur atom. This produces greater amide resonance in thioamides than in oxoamides. Model 1 predicts lower barriers in thioamides compared to oxoamides. The interaction between the nitrogen and the electron-deficient carbonyl carbon which contributes significant double-bond character to the C–N bond and stabilizes the ground state decreases when oxygen is replaced by a less electronegative sulfur atom. Also, the thioamide transition state is predicted to be more stable than the oxoamide transition state since it does not have an electron-deficient carbon atom.

Table 4 shows that increasing the size of the (thio)carbonyl substituent lowers the barrier in both oxo- and thioamides. In the case of *N,N*-dialkylamides this observation is attributed to an inability to accommodate the larger substituents in the amide plane, which results in a loss of resonance stabilization in the ground state and yields a lower rotational barrier.³⁴ The

tendency of *N*-monoalkylacetamides to prefer the conformation that places the *N*-alkyl group *syn* to the carbonyl oxygen rather than *syn* to the acetomethyl group lends support to the importance of this alkyl–alkyl steric interaction. Models 1, 2, and 3 attribute the magnitude of the internal rotation barrier to the stability of the planar ground state and are consistent with the observed trends. The thioamide barriers decrease to a greater extent as substituent bulk increases, indicating that replacement of the oxygen with the larger sulfur increases steric sensitivity in the thioamide systems. Steric repulsion in the thioamide ground state may cause greater distortions from planarity, raise thioamide ground state energy, and subsequently lower C–N rotational barriers to a greater extent than in oxoamides.

The effect of substituent electronegativity on amide rotational barriers has been studied in both the gas³⁵ and solution phase.^{36,37} In both phases, the C–N rotational barriers in the series of *N,N*-dimethylcarbamyl halides (X = Br, Cl, F) increase with halogen substituent electronegativity. The rotational barriers summarized in Tables 3–5 show the same trend in the thioamides studied, although data are limited (examination of gaseous *N,N*-dimethylthiocarbonyl bromide was not possible due to low vapor pressure at its exchange temperatures). Model 1 predicts that the transition state is destabilized by electronegative substituents since its carbon is positively charged and the barrier should increase with increasing electronegativity of the carbonyl substituent. The series Br, Cl, and F in Table 5 shows this trend for both oxoamides and thioamides, where increases in the barrier with increased halogen electronegativity are somewhat greater for the oxoamides. However, Model 1 does not explain either the lower barriers in the (thio)carbamyl halides compared to DMTF or why the thioamides (which are not characterized by a significantly electron deficient carbonyl carbon) show an analogous trend. The relatively lower barriers of the carbamyl halides compared to formamide have been previously explained by suggested contribution from resonance form III. Delocalization of the formyl lone pair on the halogen atom decreases the partial C–N double-bond character and lowers the rotational barrier.^{8,35} The contribution from resonance form III is determined by the overlap between the lone pair electrons in a 2p_z, 3p_z, or 4p_z halogen atom orbital with a carbon 2p_z orbital and the halogen atom electronegativity and therefore is expected to follow the trend Br > Cl > F. The higher barrier of DMCF may be explained by its smaller size and greater electronegativity.³⁸



Neither resonance model effectively accounts for the large decrease in $\Delta G^{\ddagger}_{298}$ when the formyl proton is replaced with a fluorine in DMTCF. Although fluorine is considerably more electronegative than hydrogen, its substitution for hydrogen in thioformamide and formamide decreases the barriers by 4.2 and 2.3 kcal mol⁻¹, respectively. Although the thioamide rotational barriers appear more sensitive to the steric properties of the thiocarbonyl group, it seems unlikely that this entirely explains the surprisingly large difference in barrier reduction between the oxo and thio fluoroamides.

Model 2 predicts the less polarized C=S bond is less affected by electronegative groups attached to carbon, and the transition state energy is not raised to the extent it is in oxoamides. Model 3 predicts that there is no significant delocalization of charge to either sulfur or oxygen in the planar ground state. The main

TABLE 6: Atomic Charges for the Ground-State Geometry Calculated Using Gaussian 94 (6-31+G*)

formamide	thioformamide	carbonyl fluoride	thiocarbonyl fluoride	carbonyl chloride	thiocarbonyl chloride
O = -0.5921	S = -0.4097	O = -0.5774	S = -0.2363	O = -0.4887	S = -0.3714
C = +0.4482	C = +0.0807	C = +1.050	C = +0.4568	C = +0.4592	C = +0.1556
N = -0.9028	N = -0.7909	N = -1.007	N = -0.8759	N = -0.8984	N = -0.7851
H = +0.1718	H = +0.2314	F = -0.3859	F = -0.2756	Cl = +0.0110	Cl = +0.0744
H = +0.4478	H = +0.4550	H = +0.4624	H = +0.4730	H = +0.4617	H = +0.4664
H = +0.4271	H = +0.4335	H = +0.4581	H = +0.4581	H = +0.4551	H = +0.4600

interaction is between carbon and nitrogen, with carbon giving up charge to nitrogen. During rotation, charge flows back from the amide nitrogen to the carbonyl carbon. Electron-withdrawing substituents on the (thio)formyl carbon would be expected to decrease the charge that it can donate to the amide nitrogen. When less charge is donated, rehybridization becomes less costly, lowering the barrier. This is the same argument used to explain the higher barriers in thioamides (over oxoamides) where the "softer" thioformyl group was said to donate more charge than the more polarized formyl group, raising the thioamide rotational barrier by making rehybridization more costly.¹⁸ This argument is not, however, compatible with the fact that electronegative substituents raise the barrier in oxoamides or that the barrier in DMCF is greater than in DMCCI.

Steric and electronic factors both influence C–N rotational barriers of acetamides and trifluoroacetamides. In the trifluoroacetamides, the positive charge on the trifluoro carbon results in a repulsive interaction with the positively charged carbonyl carbon, which should destabilize the transition state and raise ΔG^\ddagger_{298} .² Conversely, the CF_3 (4.4 Å) group is much larger than the CH_3 (3.8 Å) group, which should destabilize the ground state and lower ΔG^\ddagger_{298} . Previous gas-phase studies of dimethylamides found that ΔG^\ddagger_{298} is higher for DMCF₃ than for DMA, indicating that electronic effects are more important than steric effects.³⁵ The thioamides show a different trend. The ΔG^\ddagger_{298} of DMTCF₃ is less than that of DMTA. Steric repulsive forces between CF_3 and C=S should be greater than between CF_3 and C=O, and the lower barrier for DMTCF₃ versus DMTA indicates that steric effects predominate over electronegativity effects in these molecules.

To further explore the changes in atomic charge and polarity of the (thio)carbonyl bond when electron-withdrawing substituents are present, we performed *ab initio* calculations at the 6-31+G* level on formamide, thioformamide, carbonyl fluoride, thiocarbonyl fluoride, carbonyl chloride, and thiocarbonyl chloride. The atomic charges obtained for the geometry-optimized ground states are given in Table 6. The results show that the difference in atomic charge between the oxygen and the carbon in formamide is considerably greater than the difference in atomic charge between carbon and sulfur in thioformamide. In fact, the carbon atom in the ground state of thioformamide is essentially uncharged and the C=S bond is relatively nonpolar when compared with the polar C=O bond in amides. When the more electronegative fluorine atom is substituted for hydrogen in formamide, little change occurs in the atomic charge of the oxygen, but the carbonyl carbon is more positive. In the sulfur analog, thiocarbonyl fluoride, the atomic charge of sulfur becomes less negative and carbon's positive charge increases. The polarity of the C=S bond in thiocarbonyl fluoride is considerably less than in carbonyl fluoride, but greater than in thioformamide. Fluorine may withdraw more charge from an essentially uncharged thiocarbonyl adjacent carbon than from a positively charged carbonyl carbon. In the thioamide, this may stabilize the transition state where a full C=S bond exists and decrease the rotational barrier. Substitution of chlorine for hydrogen has less effect on atomic charges and polarity. Carbon suffers little increase in positive charge

in carbonyl chloride and chlorine takes on a slight positive charge, not inconsistent with contribution from previously suggested resonance form III. In fact, the decrease in ΔG^\ddagger_{298} due to chlorine substitution in thioamide systems may be a combined steric and electronic effect. It is also interesting to note that all of these changes have little effect on the amido hydrogens, which have a positive charge of about half an electron for all the molecules listed. Nitrogen's negative charge differs by a maximum of ca. 0.2 electron, having the greatest negative charge in carbonyl fluoride and the least in thioformamide. Nitrogen has more negative charge in the oxoamides than in the thioamides. The *ab initio* results are consistent with the smaller effect of electron-withdrawing substituents on thioamides and on the decrease in the rotational barrier when CF_3 is substituted for CH_3 in DMTA. We hypothesize that the smaller positive charge on the thiocarbonyl carbon renders the mechanism responsible for destabilization of the transition state much less important in thioamides.

In conclusion, these results suggest that the rotational barrier in *N,N*-dimethylthioamides is extremely sensitive to the steric features of the thiocarbonyl substituent. Furthermore, it is the relative nonpolarity of the C=S moiety and the neutrality of the thiocarbonyl carbon that are important in determining the effect of electronegative substituents. Work in progress examines the effect of inductive substituents at both the carbonyl (thiocarbonyl) and nitrogen positions in amides and thioamides.

Acknowledgment. We are pleased to acknowledge the National Science Foundation (CHE 93-21079) for support of this research. C.B.L. also thanks the Idaho State Board of Education for support from Specific Research Grant S96-086.

References and Notes

- (1) Lehninger, A. L.; Nelson, D. L.; Cox, M. M. *Principles of Biochemistry*; Worth: New York, 1993.
- (2) Wiberg, K. B.; Hadad, C. M.; Rablen, P. R.; Cioslowski, J. *J. Am. Chem. Soc.* **1992**, *114*, 8644.
- (3) Stewart, W. E.; Sidall, T. H., III. *Chem. Rev.* **1970**, *70* (5), 517.
- (4) Oki, M. *Applications of Dynamic NMR Spectroscopy to Organic Chemistry*; VCH: Deerfield Beach, FL, 1985.
- (5) Berg, U.; Blum, Z. *J. Chem. Res.* **1983**, 206.
- (6) Drakenberg, T. *J. Phys. Chem.* **1976**, *80*, 1023.
- (7) Feigel, M. *J. Phys. Chem.* **1983**, *87*, 3054.
- (8) Neuman, R. C., Jr.; Rourke, D. N.; Jonas, V. *J. Am. Chem. Soc.* **1967**, *89*, 3412.
- (9) Hobson, R. F.; Reeves, L. W.; Shaw, K. N. *J. Phys. Chem.* **1973**, *77*, 1228.
- (10) Sandstrom, J. *J. Phys. Chem.* **1967**, *71*, 2318.
- (11) Piccinni-Leopardi, C.; Omer, F.; Zimmerman, D.; Reisse, J. *Can. J. Chem.* **1977**, *55*, 2649.
- (12) Berg, U.; Grimaud, M.; Sandstrom, J. *Nouv. J. Chim.* **1979**, *3*, 175.
- (13) Sidall, T. H., III; Stewart, W. E.; Knight, F. D. *J. Phys. Chem.* **1970**, *74*, 3580.
- (14) Walter, W.; Schaumann, E.; Rose, H. *Org. Magn. Reson.* **1973**, *5* (4), 191.
- (15) Isaksson, G.; Sandstrom, J. *Acta Chem. Scand.* **1967**, *21*(6) 1605.
- (16) Abboud, J. L. M.; Mo', O.; de-Paz, J. L. G.; Yanez, M.; Esseffar, M.; Bouab, W.; El-Mouhtadi, M.; Mokhlisse, R.; Ballesteros, E.; Herreros, M.; Homan, H.; Lopez-Mardomingo, C.; Notario, R. *J. Am. Chem. Soc.* **1993**, *115*, 12468.
- (17) Wiberg, K. B.; Rablen, P. R. *J. Am. Chem. Soc.* **1995**, *117*, 2201.
- (18) Laidig, K. E.; Cameron, L. M. *J. Am. Chem. Soc.* **1996**, *118*, 1737.
- (19) Feigel, M.; Strassner, T. *J. Mol. Struct.* **1993**, *283*, 33.

- (20) Walter, W.; Imbert, J. P. *J. Mol. Struct.* **1975**, 29, 253.
- (21) Lim, K.-T.; Francl, M. M. *J. Phys. Chem.* **1987**, 91, 2716.
- (22) Suarez, C.; LeMaster, C. B.; LeMaster, C. L.; Tafazzoli, M.; True, N. S. *J. Phys. Chem.* **1990**, 94, 6679.
- (23) Goshorn, R. H.; Lewis, W. W., Jr.; Jaul, E.; Ritter, E. *J. Org. Synth.* **1955**, 35, 551.
- (24) Wagner, R. B.; Zook, H. D. *Synthetic Organic Chemistry*; Wiley: New York, 1953.
- (25) (a) Stephenson, D. S.; Binsch, G. Program No. 365. (b) LeMaster, C. B.; LeMaster, C. L.; True, N. S. Programs No. 569 and QCMP059. Quantum Chemistry Program Exchange, Indiana University, Bloomington, IN 47405.
- (26) Ross, B. D.; True, N. S.; Decker, D. L. *J. Phys. Chem.* **1983**, 87, 89.
- (27) Previous unpublished results for *N,N*-dimethylpropionamide showed temperature-independent magnetic equivalence of the dimethylamino proton resonances in the gas phase. This is consistent with the result obtained for *N,N*-dimethylformamide (DMF). Gas-phase activation parameters for DMF were obtained from ^{13}C NMR spectra. See: Ross, B. D.; True, N. S. *J. Am. Chem. Soc.* **1984**, 106, 2451.
- (28) Ou, M.-C.; Chu, S.-Y. *J. Phys. Chem.* **1995**, 99, 556.
- (29) Jackman, J. L. In *Dynamic Nuclear Magnetic Resonance Spectroscopy*; Jackman, L. M., Cotton, F. A., Eds.; Academic Press: New York, 1975; pp 203–252, and references therein.
- (30) LeMaster, C. B.; True, N. S. *J. Phys. Chem.* **1989**, 93, 1307.
- (31) True, N. S.; Suarez, C. *Advances in Molecular Structure Research*; JAI: London, 1995; Vol I. p 115.
- (32) Suarez, C.; LeMaster, C. B.; LeMaster, C. L.; Tafazzoli, M.; True, N. S. *J. Phys. Chem.* **1990**, 94, 6679.
- (33) Ross, B. D.; True, N. S.; Matson, G. B. *J. Phys. Chem.* **1984**, 88, 2675.
- (34) Wiberg, K. B.; Rablen, P. R.; Rush, D. J.; Keith, T. A. *J. Am. Chem. Soc.* **1995**, 117, 4261.
- (35) Ross, B. D.; Wong, L. T.; True, N. S. *J. Phys. Chem.* **1985**, 89, 836.
- (36) Allan, E. A.; Hobson, R. F.; Reeves, L. W.; Shaw, K. N. *J. Am. Chem. Soc.* **1972**, 94, 6604.
- (37) Reeves, L. W.; Shaw, K. N. *Can. J. Chem.* **1971**, 49, 3672.
- (38) The diameter of the CF_3 group is 4.4 Å and of the CH_3 3.8 Å, as estimated from AMPAC results using the AM1 Hamiltonian. Program No. 506, Quantum Chemistry Program Exchange, Indiana University, Bloomington, IN 47405.
- (39) *Beilstein*, 4th ed., Springer-Verlag: Berlin, 1958; Vol. 1, Suppl. 3, p 161.
- (40) Pines, A.; Rabinovitz, M. *Tetrahedron Lett.* **1968**, 3529.
- (41) Fryer, C. W.; Conti, F.; Franconi, C. *Ric. Sci., Parte 2: Sez. A*, **1965**, 8, 788.
- (42) Neuman, R. C., Jr.; Young, L. B. *J. Phys. Chem.* **1965**, 69, 2570.
- (43) Sunners, B.; Piette, L. H.; Schneider, W. G. *Can. J. Chem.* **1960**, 38, 681.
- (44) Rogers, M. T.; Woodbrey, J. C. *J. Phys. Chem.* **1962**, 66, 540.
- (45) Reeves, L. W.; Shaddick, R. C.; Shaw, K. N. *Can. J. Chem.* **1971**, 49, 3683.
- (46) Neuman, R. C., Jr.; Jonas, V. *J. Am. Chem. Soc.* **1968**, 90, 1970.
- (47) Ross, B. D.; True, N. S. *J. Am. Chem. Soc.* **1984**, 106, 2451.
- (48) Drakenberg, T.; Dahlquist, K.; Forsen, S. *J. Phys. Chem.* **1972**, 76 (15), 2178.
- (49) Woodbrey, J. C.; Rogers, M. T. *J. Am. Chem. Soc.* **1962**, 84, 13.